12

Records of Magnetic Fields in the Chondrule Formation Environment

ROGER R. FU, BENJAMIN P. WEISS, DEVIN L. SCHRADER, AND BRANDON C. JOHNSON

Abstract

Chondrules contain ferromagnetic minerals that may retain a record of the magnetic field environments in which they cooled. Paleomagnetic experiments on separated chondrules can potentially reveal the presence of remanent magnetization from the time of chondrule formation. The existence of such a magnetization places quantitative bounds on the frequency of inter-chondrule collisions, while the intensity of magnetization may be used to infer the strength of nebular magnetic fields and thereby constrain the mechanism of chondrule formation. Recent advances in laboratory instrumentation and techniques have permitted the isolation of nebular remanent magnetization in chondrules, providing the potential basis to probe the formation environments of chondrules from a range of chondrite classes.

12.1 Introduction

Chondrules are millimeter-scale, nearly spherical igneous inclusions found in chondritic meteorites (chondrites). Their abundance in chondrites and early crystallization within several million years (My) of the formation of calcium aluminum-rich inclusions (CAIs) suggests that they may have played an important role in the formation of solid bodies in the solar system [e.g., Villeneuve et al. (2009); Kita and Ushikubo (2012); Schrader et al. (2017)]. However, fundamental questions about the origin of chondrules remain unanswered, including the mechanism of formation and the spatial distribution of chondrule formation regions in the solar nebula.

Paleomagnetism is a technique that takes advantage of naturally occurring ferromagnetic minerals in rocks to infer the presence and intensity of ancient magnetic fields. Although only a handful of paleomagnetic studies to date have measured separated, individual chondrules, information about magnetic fields during chondrule formation may yield valuable information about their formation environment. Interactions with the partially ionized nebular gas caused the embedded magnetic fields to vary in time and position in the solar nebula (Balbus, 2003; Wardle, 2007; Bai, 2016), permitting knowledge of the magnetic field to constrain potentially the timing and location of chondrule formation. Furthermore, proposed chondrule formation models predict a range of magnetic field strengths during the formation event, implying that paleomagnetic inferences of paleofield intensity may help to identify the mechanism or mechanisms of chondrule formation. Finally, although beyond the scope of this chapter, paleomagnetic experiments on

chondrules may reveal the strength of background nebular magnetic fields, which likely played a significant role in disk evolution and planet formation (Fu et al., 2014b).

In this chapter, we begin by outlining the potential contributions of paleomagnetism to questions about chondrule formation. We then turn to a review of existing paleomagnetic studies on individual chondrules, highlighting the significant challenges posed by sample selection and by the measurement of small, weakly magnetized samples.

12.2 The Potential of Chondrule Paleomagnetism

12.2.1 Implications of a Preserved Magnetization

Paleomagnetic constraints on the chondrule formation environment come from two observables related to the chondrules' natural remanent magnetization (NRM), the semipermanent alignment of electron spins within ferromagnetic materials imparted by past magnetic fields. First, the existence of any identifiable, linear component of NRM places requirements on the stability of the magnetic field in the chondrule's frame of reference (Figure 12.1). Second, the intensity of chondrule NRM may be used to infer the strength of background magnetic fields during the formation process. In both cases, the recorders of ancient magnetic fields within chondrules are inclusions of ferromagnetic minerals such as magnetite, pyrrhotite, and FeNi alloys including kamacite, martensite, taenite, and tetrataenite (Uehara et al., 2011). Among these, FeNi alloys and, in some chondrule groups, pyrrhotite are most likely to have a nebular origin and record the magnetic field during chondrule formation (Krot et al., 1998; Schrader et al., 2016a). Similar to igneous rocks on Earth and other solar system bodies, the form of NRM carried by

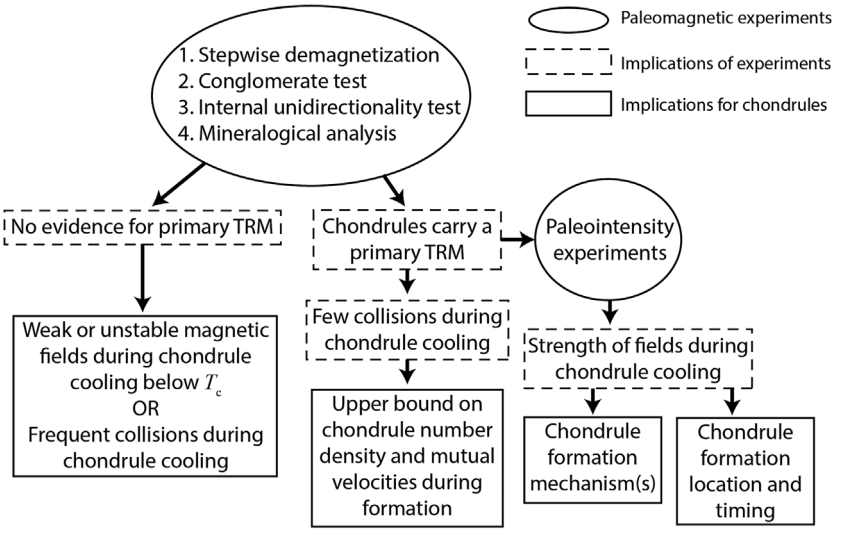

Figure 12.1 Schematic summary of potential constraints on chondrule formation derived from paleomagnetic experiments. Abbreviation T_c refers to Curie temperature, which is 780 °C for the native Fe mineral kamacite.

ferromagnetic grains in chondrules may be a thermoremanent magnetization (TRM) if their cooling at temperatures below the Curie point (700–780 °C for typical FeNi compositions) took place in a directionally stable background magnetic field (Swartzendruber et al., 1991; Kimura et al., 2008). We refer to such a magnetization as a primary natural remanent magnetization (primary NRM), meaning that its acquisition occurred during the formation of the chondrule and distinguishing it from secondary NRM acquired during thermal and/or aqueous alteration events in the chondrule's subsequent history.

Laboratory demagnetization of separated chondrules via heating or room temperature alternating field (AF) protocols are designed to remove secondary overprints and isolate the primary component of magnetization, if any. For a primary NRM to be properly recognized as a component of magnetization, the primary NRM must display a consistent direction during demagnetization after removal of any secondary magnetization components (Tauxe, 2010). During thermal demagnetization, the temperatures over which the observed sample magnetization trends in a consistent direction is known as the blocking temperature range of that magnetization component. For a chondrule to carry such an identifiable magnetization component, the background magnetic field must have remained constant with respect to the chondrule or, for a rotating chondrule, the chondrule's angular momentum axis during cooling over the blocking temperature range. In the latter case, a spinning or precessing chondrule is expected to record a component of magnetization parallel to its angular momentum axis (Fu et al., 2014b; Takac and Kletetschka, 2015).

The identification of a primary NRM in a population of chondrules therefore implies that these specimens must have avoided significant reorientation of their angular momentum vectors as they cooled through the observed range of blocking temperatures for the primary NRM, which can be quantified using stepwise thermal demagnetization. The initial rotation rate of chondrules during cooling above the solidus was likely in excess of 100 rad s^{-1} based on their three-dimensional shapes (Tsuchiyama et al., 2003; Miura et al., 2008). Under minimum mass solar nebula conditions [MMSN; (Hayashi, 1981)], the frictional decay of angular velocity for a 1-mm diameter chondrule takes place over the course of several hours at 1 AU and over 10^3 hours at 10 AU (Fu and Weiss, 2012). Other solar nebula models predict gas densities and nebular temperatures that vary by a factor of ~2 and ~4 from the MMSN, respectively, while gas density may have declined by more than an order of magnitude within 3–4 My after CAIs (Bitsch et al., 2015; Wang et al., 2017). As such, the spin-down timescales calculated above are likely to represent lower bounds during the time period of peak chondrule formation between 2 and 3 My after CAIs. Given chondrule cooling rates of 10–1,000 °C h^{-1} (Hewins et al., 2005; Tachibana et al., 2006; Schrader et al., 2016b), these spin-down rates imply that chondrules are expected to be spinning during most or all of the cooling process assuming background nebular gas densities, especially in the outer solar system. Given these rotation rates, random collisions with gas molecules during the spin-down process impart negligible changes to the rotation state, equivalent to ~0.01 rad s^{-1} for a 1 mm diameter chondrule at 1 AU (Fu et al., 2014b). Therefore, a spinning chondrule cooling in the gas environment of the solar nebula is expected to retain a nearly constant angular momentum vector orientation, permitting the acquisition of a primary NRM if a significant magnetic field is present.

Enhancement in nebular gas density of several orders of magnitude would not affect this expectation in the outer solar system at 2–3 My after CAIs. On the other hand, early formation

of chondrules in the inner solar system (<2 AU) combined with local enhancement of gas densities during chondrule formation may result in chondrules that de-spin completely before sufficient cooling to record ambient magnetic fields. In such cases, the orientation of the chondrule in space may undergo Brownian motion due to collisions with gas molecules, resulting in non-unidirectional magnetization.

On the other hand, collisions with other chondrules would dramatically change the angular momentum of a cooling chondrule. If such collisions occurred frequently during the cooling process below the Curie temperature, then chondrules would not be able to record an identifiable primary NRM. The observation of a primary NRM in a chondrule would therefore imply an upper bound on the probability of interchondrule collisions during the interval of cooling corresponding to TRM acquisition. For a collection of equal-sized spherical particles with radius r_c moving with mutual velocity v_c, the expected number of collisions (N) experienced by a single particle in time Δt is given by $N = 4\pi r^2 v_c n \Delta t$, where n is the number density of particles (Ciesla et al., 2004). The parameter Δt may be estimated by combining the temperature interval of remanence acquisition observed from thermal demagnetization and subsilicate solidus cooling rates derived from petrographic observations. To constrain cooling rates at temperatures below the 780 °C Curie point of kamacite, we use the texture and compositions of sulfides in some minimally altered chondrite groups. The morphology, texture, and equilibration temperature of these phases indicate formation at high temperatures during chondrule cooling and rule out a low temperature origin on the parent asteroids (Schrader et al., 2015, 2016a, 2016b). The existence of a primary NRM in a population of chondrules, which constrain N, therefore constrains the number density and velocity of chondrules (Figure 12.1), analogous to observations of compound chondrule frequency.

Finally, even in the case of a consistent rotation axis, chondrules would not record a primary NRM if the background magnetic field direction were unstable during the cooling time window. Therefore, the detection of a primary NRM implies that the local magnetic field remained constant in direction for at least the several hours during which the chondrule cooled through the block temperature range.

12.2.2 Implications of the Paleointensity

If and when a primary NRM is identified in a chondrule, further paleomagnetic experiments may be able to infer the paleointensity, or the strength of the ancient magnetic field during TRM acquisition (Figure 12.1). The most prevalent paleointensity protocols impart an artificial remanent magnetization in a known laboratory field using a variety of both high temperature and room temperature techniques (Tauxe, 2010). By comparing the strengths of the natural and artificial remanence magnetizations, the approximate strength of the original natural magnetic field may be deduced. Similar to other extraterrestrial samples, ferromagnetic phases in chondrules often experience severe chemical alteration during laboratory heating. As such, paleointensity estimates on single chondrules are typically based on room temperature methods that are uncertain by a 2-standard deviation factor of 3–5 [see discussion in Weiss and Tikoo (2014)]. In the best-case scenario where laboratory cooling experiments are available as calibrations for room temperature paleointensities (Lappe et al., 2013), this uncertainty may be reduced to a

factor of ~1.3. As a second source of uncertainty, chondrule rotation during cooling implies that the recorded paleointensity would be attenuated by a factor cos θ, where θ is the angle between the rotation axis and the magnetic field. Although the factor cos θ is unknown for any one chondrule, the mean value across a population of randomly oriented chondrules approaches 0.5 in the limit of a large sample size (Fu et al., 2014b). The experimental and sample selection challenges of chondrule paleomagnetism limit the practical sample size, leading to uncertainty on the multiplier used to correct for chondrule rotation.

Together, these uncertainties imply that chondrule-derived paleointensities are accurate to an order of magnitude in the absence of calibrations against a laboratory TRM and to a factor of 1.5 in the best-case scenario where such experiments are available (Fu et al., 2014b). With these limitations in mind, paleomagnetic constraints on field intensity during chondrule formation may be able to distinguish between different formation mechanisms that predict significantly different field intensities.

Fortunately, existing models indeed place chondrule formation in broadly disparate magnetic field environments. The *x*-wind model of chondrule formation places the site of chondrule formation between approximately 0.1 and 0.5 AU from the sun, resulting in exposure to strong magnetic fields. Chondrules traveling in the magnetocentrifugal winds invoked by the *x*-wind model experience relatively constant magnetic fields of 400–800 μT during cooling between the 780 °C Curie point of kamacite and 300 °C, assuming chondrule formation during the embedded phase of the protosun (Shu et al., 1996, 1997). These field values drop to 80–160 μT for chondrule formation during the revealed phase.

Models that place chondrule formation in the protoplanetary disk itself make chondrule paleointensity predictions that depend on the local nebular magnetic field strength. The variation of nebular field strength with orbital radius is complex and model-dependent. Within 5–10 AU of the sun, higher concentrations of dust grains and higher optical depths at the disk midplane may lead to the formation of a "dead zone," in which magnetic field strengths are suppressed due to low gas ionization levels (Gammie, 1996; Turner and Sano, 2008; Bai, 2011). However, recent simulations that more fully incorporate nonideal magnetohydrodynamical (MHD) phenomena including the Hall effect suggest that significant magnetic fields may persist in the dead zone [Figure 12.2; (Bai, 2014; Lesur et al., 2014)]. At the same time, the regions of anomalous low or high gas density, which may affect local magnetic field strength, have been observed in other protoplanetary disks and may have formed with or without the presence of planets (van der Marel et al., 2013; Zhu, Stone, and Rafikov, 2013; Flock et al., 2015). However, the advection of magnetic fields into these regions may result in minimal change in the magnetic field strength even in zones of lower gas density (Wang et al., 2017). Finally, the inferred dissipation of the nebular gas at least in specific regions of the disk by ~3–4 My after CAIs (Bitsch et al., 2015; Wang et al., 2017) implies that the strength of nebular magnetic fields may have evolved rapidly on $\leq$1 My timescales. As such, accurate geochronology of chondrules, preferably on the same specimens being analyzed for paleomagnetism, is critical for the interpretation of paleomagnetic results.

Despite these uncertainties, an order-of-magnitude theoretical estimate of background nebular field strengths may be derived under the assumption that magnetic fields led to the bulk of angular momentum transport at all radii in the protosolar disk. In this scenario, the magnetic field strength is a function of the assumed mechanism of transport and accretion rate and

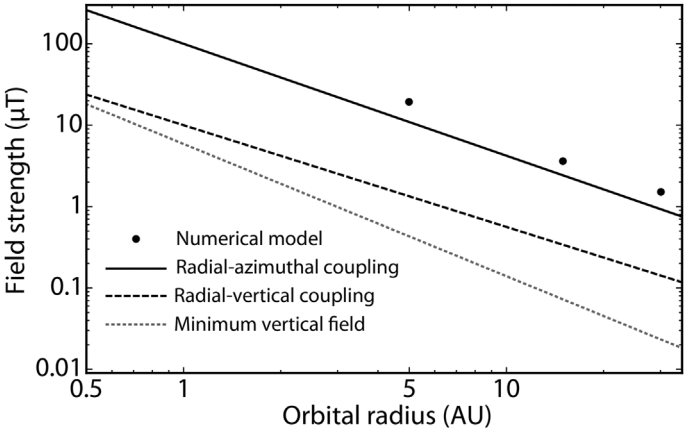

Figure 12.2 Model predictions for background nebular magnetic field intensities. Points at 5, 15, and 30 AU denote the approximate maximum midplane field intensities observed in numerical MHD simulations that fully include nonideal MHD effects (Bai, 2015). Because the modeled field strengths fluctuate in time, these peak values may be regarded as upper bounds on the field strength. Solid line denotes the magnetic field intensities required to produce a mass accretion rate of 10^{-8} $M_{\odot}$ y^{-1} assuming accretion by coupling of the radial and azimuthal components of the magnetic field [(Bai and Goodman, 2009); Equation 16]. Dashed line shows the magnetic field intensities for the same accretion rate but assuming accretion by radial-vertical magnetic field coupling [(Bai and Goodman, 2009); Equation 7]. Dotted gray line denotes the minimum, nonfluctuating net vertical magnetic field strength needed to produce the above accretion rate according to numerical MHD simulations (Bai, 2015). This value may be regarded as a lower bound on the midplane field intensity. Physical field strengths from numerical simulations are computed by combining Equation 14 of Bai (2015) and the definition of the plasma β parameter for a MMSN scenario.

decreases with radius following a power-law [Figure 12.2; (Wardle, 2007; Bai and Goodman, 2009)]. Assuming a typical sun-like protostellar accretion rate of 10^{-8} solar masses per year ($M_{\odot}$ y^{-1}), the background nebular field strength at 1 AU is between 5 and 100 μT, which declines to 0.02–1 μT at 30 AU. These field strengths are consistent with estimates assuming a turbulent, one-dimensional disk (Guilet and Ogilvie, 2014) and with numerical MHD simulations (Bai, 2014) assuming net vertical fields of ~10 μT at 1 AU. Although the value of the net vertical field is not known directly, a ~10 μT value is in agreement with estimates from models of magnetic field diffusion in the protoplanetary disk (Desch and Mouschovias, 2001; Okuzumi et al., 2014).

The magnetic field intensity potentially recorded in chondrules formed in the protoplanetary disk is a function of these background magnetic field intensities as well as any modification due to the chondrule formation mechanism itself. The degree of field amplification by local hydrodynamic processes depends on the magnetic diffusivity of the gas and the size of the region of interest. For the impact formation model of chondrules, the spatial scale of the chondrule-forming jets is $\leq 10^5$ km. The presence of dust particles leads to very low ionization fractions ($<10^{-18}$) for nebular gas near the disk midplane, corresponding to high magnetic diffusivities on the order of 10^{18}–10^{20} m^2 s^{-1} (Wardle, 2007). The $\leq$780 °C temperatures in which magnetic fields may be recorded by chondrules are unlikely to lead to significant thermal ionization (McNally et al., 2013), while the enhanced solids concentration may lead to even higher magnetic diffusivities. Under these conditions, magnetic fields are expected to diffuse

across the thickness of chondrule-forming outflows in less than 1 s (Asphaug et al., 2011; Johnson et al., 2015). Chondrules formed in planetesimal collisions would therefore experience no enhancement of the background nebular magnetic field, predicting recorded paleointensities of 0.02–100 μT, depending on the location in the protoplanetary disk (Figure 12.2).

In the case of the nebular shock model of chondrule formation, compression of the nebular gas over potentially large spatial scales may prevent the rapid diffusion of magnetic fields, resulting in enhancement of the nebular magnetic field by a factor of approximately 10 (Desch and Connolly, 2002). As such, predicted recorded paleointensities for chondrules formed via this mechanism are in the 100–1,000 μT range in the innermost disk around 1 AU, overlapping with fields expected for the *x*-wind model. Meanwhile, shock-enhanced field strengths in and beyond the asteroid belt are between 1 and 100 μT.

Two other hypothesized mechanisms of chondrule formation, the magnetic reconnection flare and short circuit instability models (Levy and Araki, 1989; McNally et al., 2013), predict potentially very high local magnetic field strengths of 500 and 10^4 μT, respectively, during the peak heating phase of chondrule formation. However, these strong magnetic fields may decay significantly by the time temperature drops below the 780 °C Curie temperature of kamacite. More detailed modeling of the simultaneous decay of magnetic field strength and temperature is required to produce quantitative paleointensity predictions for chondrules formed in these mechanisms.

12.3 Previous Paleomagnetic Experiments on Chondrules

Several basic properties of chondrules pose formidable challenges to their paleomagnetic characterization. The small size and nearly spherical morphology of chondrules have created difficulties for the accurate measurement of their magnetic moment and for the preparation of mutually oriented samples. As importantly, the complex, protracted, and often poorly known geological histories of chondrules in the solar nebula, on their asteroidal parent bodies, and on Earth result in a wide range of secondary processes that may have potentially resulted in partial or complete remagnetization. As a result of these challenges, few robust paleomagnetic measurements of individual chondrules have been obtained, and even fewer among these can provide meaningful constraints on the chondrule formation process itself.

A critical experiment used to determine the origin of chondrule NRM is the paleomagnetic conglomerate test. In this analysis, consistent magnetization directions found in multiple, mutually oriented chondrules indicates that the magnetization postdates the assembly of the meteorite and therefore is not a primary record of magnetic fields in the solar nebula during chondrule formation. The paleomagnetic conglomerate test can only be performed on chondrules whose mutual orientations are maintained through the extraction process.

The earliest paleomagnetic experiments on separated chondrules focused on unoriented specimens from the Allende CV3 carbonaceous chondrite (Lanoix et al., 1978). Paleointensity experiments using a heating-based protocol suggested very high paleointensites of 1,600 μT over a blocking temperature range of 350–500 °C. However, because the chondrules in these experiments lacked mutual orientation, the authors could not rule out a late remagnetization event during processing on the parent body or due to exposure to strong artificial magnetic fields on Earth. Indeed, the very high inferred paleointensities are suggestive of contamination due to

hand magnet magnetic fields (Wasilewski, 1981; Weiss et al., 2010). As further evidence that the chondrule paleointensities obtained by Lanoix et al. (1978) were the result of anomalous hand magnet contamination, a follow-up study of mutually oriented Allende chondrules by the same research group did not find such high paleointensities in magnetization over the same blocking temperature range (Sugiura et al., 1979). Instead, the later study obtained a paleointensity of ~100 μT on a different component of magnetization blocked below 300 °C. Because the direction of this lower temperature magnetization was consistent among different chondrules and with matrix samples, it must have been acquired after the accretion of the parent body and cannot constrain preaccretional fields during chondrule formation (Carporzen et al., 2011).

As such, early published nebular field intensities of 100–>1,000 μT based on the Lanoix et al. (1978) work [e.g., Levy and Sonett (1978)] should be disregarded. Furthermore the ~100 μT paleointensity of CV parent body magnetic fields obtained by Sugiura et al. (1979) has been mistakenly cited by later studies as corresponding to the nebular magnetic field [e.g., Levy and Araki (1989); Stepinski (1992); Shu et al. (1996); Nübold and Glassmeier (2000); Johansen (2009)]. Finally, other early paleointensities derived from unoriented chondrules, such as the values of up to ~1,000 μT obtained from the Allende, Allegan (H5), Bjurböle (L/LL4), and Chainpur (LL3.4) chondrites, were also likely influenced by contamination from exposure to hand magnets (Wasilewski and O'Bryan, 1994). To identify similar contamination by hand magnets, future studies of meteorite paleomagnetism should evaluate the ratio of NRM to isothermal remanent magnetization (IRM), which is anomalously high for samples exposed to strong fields (Weiss et al., 2010). Furthermore, the measurement of mutually oriented samples that include fusion crust material would aid in the confident detection of hand magnet-induced overprints, which affect the fusion crust and are expected to be heterogeneous in strength and direction (Weiss and Elkins-Tanton, 2013).

Later studies of mutually oriented chondrules from Allende have revealed ostensible evidence that a primary NRM recording chondrule formation magnetic fields may be preserved. Sugiura et al. (1979) and Sugiura and Strangway (1985) showed that a high temperature component of magnetization blocked above ~300 °C in Allende chondrules passes the paleomagnetic conglomerate test (i.e., random magnetization directions suggesting preaccretional origin). Motivated by these findings, Fu et al. (2014a) performed additional experiments demonstrating that, while chondrules separated from Allende indeed exhibit distinct magnetization directions, *subsamples* of chondrules also showed randomized magnetizations (Figure 12.3a). These random magnetization directions within a single chondrule sum up to an overall random direction for the chondrule, thereby explaining the positive conglomerate test but invalidating the inference that the magnetization predates accretion. Such heterogeneity at <1-mm length scales is not consistent with a primary NRM acquired during chondrule cooling. At the same time, high-resolution magnetic mapping shows that magnetization in Allende chondrules is associated closely with altered mesostases [Figure 12.4; Glenn et al. (2017)], which formed after parent body accretion. These lines of evidence indicate that the non-unidirectional magnetization in Allende chondrules was acquired in the presence of a weak magnetic field during or after aqueous alteration on the CV parent body.

The misidentification of a parent body magnetic record in Allende chondrules as a primary nebular NRM highlights the importance of measuring subsamples of individual chondrules to

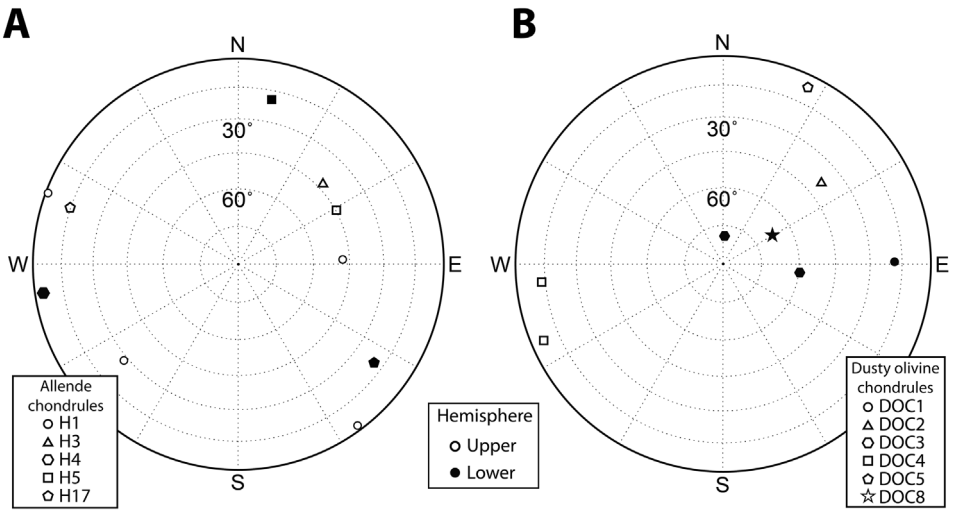

Figure 12.3 Equal area stereonet projections showing contrasting magnetization distributions in chondrules and chondrule sub-samples from the (a) Allende and (b) Semarkona meteorites. Data points represent the direction of high temperature or high coercivity magnetization of the indicated sample plotted using a Lambert equal-area projection where hollow (solid) symbols correspond to the upper (lower) hemispheres. Samples from each meteorite are mutually oriented. Note that subsamples of Allende chondrules show random directions, while dusty olivine-bearing chondrules from Semarkona have internally consistent directions.

avoid the possibility of a false-positive conglomerate test resulting from locally randomized magnetizations. As importantly, careful identification of the mineralogical basis of magnetization is necessary to distinguish a primary NRM from the product of later remagnetization.

Motivated in part by the latter requirement, recent experiments on chondrules from the Semarkona LL3.00 ordinary chondrite have focused on dusty olivine grains, which contain micrometer to submicrometer grains of Fe-metal exsolved from Fe-bearing olivine during primary cooling of the chondrules under relatively reducing conditions (Jones and Danielson, 1997; Leroux et al., 2003). Because these Fe-metal grains are situated within the host olivine, they are effectively shielded from the aqueous alteration that has severely affected the matrix and chondrules of most weakly metamorphosed chondrites of petrologic type 3 and lower (Uehara and Nakamura, 2006). As a further advantage of studying dusty olivine-bearing chondrules, experiments on artificially synthesized dusty olivines have permitted calibrations of room-temperature paleointensity protocols with accuracies of ~30 percent (Lappe et al., 2013), which is a dramatic improvement over typical uncertainties of several hundred percent associated with these methods (see Section 12.2.2).

To test the primary origin of dusty olivine magnetization in Semarkona, Fu et al. (2014b) performed a conglomerate test using eight chondrules, and, furthermore, divided two chondrules into two subsamples each to test the internal unidirectionality of magnetization. Five of the seven dusty olivine-bearing chondrules subjected to AF demagnetization carried identifiable, origin-trending, high-coercivity components. Such magnetizations are likely to have a

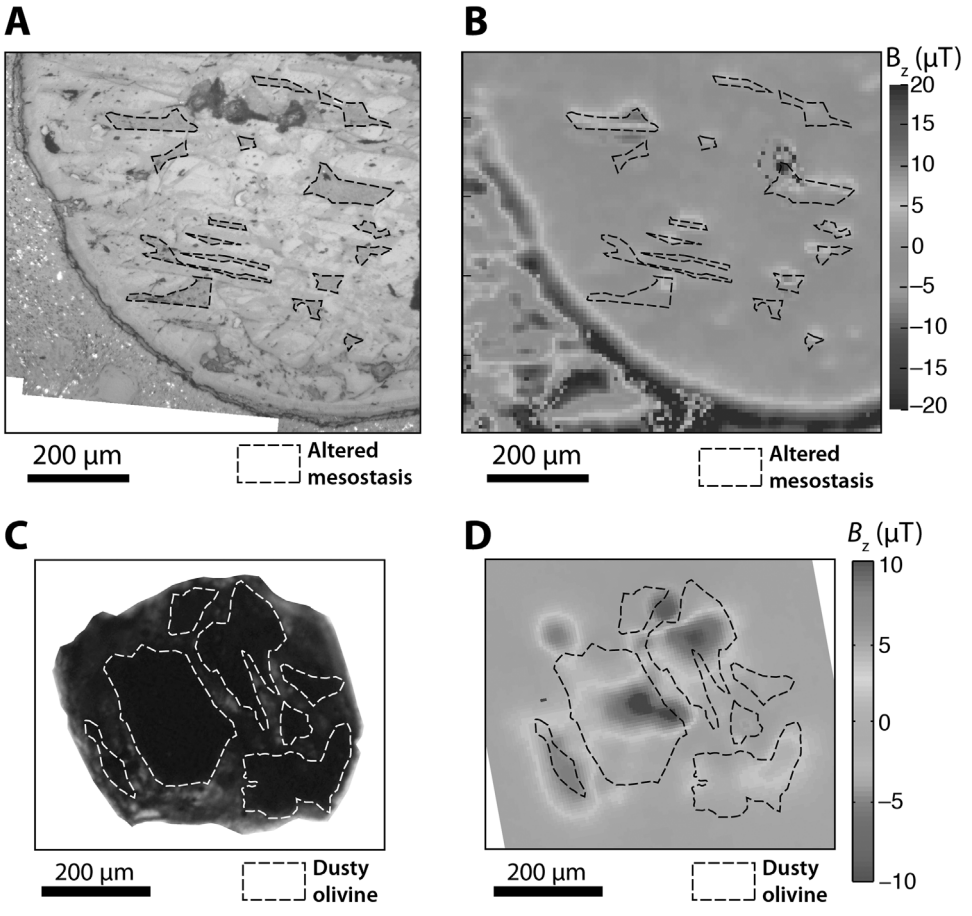

Figure 12.4 Optical and magnetic microscopy of chondrules from the Allende and Semarkona meteorites. (a) Reflected light optical photomicrograph showing a barred olivine chondrule in Allende with altered mesostasis regions highlighted. (b) Quantum diamond microscope (QDM) map of magnetic fields due to a near-saturation isothermal remanent magnetization (IRM) in the upward, in-plane direction. Note the correspondence between magnetic sources and altered mesostasis. (c) Transmitted light photomicrograph of a dusty olivine-bearing chondrule from Semarkona with dusty olivine regions highlighted. (d) QDM map of magnetic fields due to an out-of-plane IRM. Note the spatial correspondence between magnetic sources and dusty olivines, which were formed during chondrule formation and permit the preservation of a primary NRM. Images in panels (a) and (b) are after Glenn et al. (2017). Images in panels (c) and (d) are after Fu et al. (2014b). (A black-and-white version of this figure will appear in some formats. For the colour version, please refer to the plate section.)

primary origin because their high-coercivity carrier grains are difficult to remagnetize, while their origin-trending directions imply that no higher-coercivity, and therefore higher-stability, magnetization exists in the sample. Meanwhile, thermal demagnetization of one dusty olivine-bearing chondrule isolated a high temperature component of magnetization that is blocked between 400 and $\geq$600 °C. Given that the cooling timescale in the laboratory (~5 min) is much

shorter than the timescale of chondrule formation (several hours), these laboratory unblocking temperatures correspond to temperatures during natural chondrule cooling of 360 °C and ≥580 °C, respectively (Garrick-Bethell and Weiss, 2010). Such a temperature range is fully consistent with a primary NRM carried by Fe-metal that was subsequently partially demagnetized during parent body metamorphism at ~200 °C for ~1 My. Similar to the Allende chondrules discussed above, the magnetization directions of individual chondrules are randomly distributed (Figure 12.3b). However, subsamples of single Semarkona chondrules showed consistent magnetization directions. This critical piece of evidence strongly suggests that dusty olivine-bearing chondrules in Semarkona, unlike chondrules in Allende, preserve a primary NRM recorded in the solar nebula during chondrule cooling.

Room temperature paleointensity experiments on five dusty olivine-bearing chondrules from Semarkona yielded a raw mean of 27 μT, which resulted in a final chondrule cooling field intensity estimate of 54 ± 21 μT, assuming continuous rotation of chondrules around a single axis during cooling. The formation location of our measured chondrules in the protoplanetary disk is poorly known and depends on the extent of radial migration both before and after accretion. Assuming Semarkona chondrules were formed in the protoplanetary disk at between 2 and 3 AU corresponding to the modern asteroid belt, this paleointensity is consistent with both the impact and shock wave models for chondrule formation but is likely too low to be compatible with the *x*-wind model.

The existence of inferred primary NRM in six out of eight Semarkona dusty olivines suggests that approximately 75 percent of chondrules avoided reorientation of their spin axes due to interchondrule collisions during cooling across the 360–≥580 °C unblocking temperature range. We therefore estimate the number density of chondrules during formation (see Section 12.2.1) assuming a collision probability of 0.25, a cooling rate of ~100 °C h^{-1} inferred for the 600–400 °C cooling interval (Schrader et al., 2016b), and uniform chondrule diameters of 0.5 mm corresponding to the dusty olivine-bearing specimens. Estimates of mutual velocities among chondrules vary widely between approximately 0.001 and 1 m s^{-1} (Cuzzi and Hogan, 2003; Carrera et al., 2015), where the higher value is a mean mutual velocity due to high levels of nebular turbulence (α parameter of 10^{-2}) and the lower value is based on a maximum likelihood analysis of particles with similar mean mutual velocities, but considering only particles located close to each other. Higher concentrations of solids in the chondrule formation region may have resulted in correlated motions and even lower mutual velocities. Future models of chondrule mutual velocities that consider in detail the feedback between particle and gas motion [e.g., (Johnson et al., 2015)] are required to create more robust estimates of chondrule collision rates.

Adopting the collision probability inferred from chondrule paleomagnetism measurements, the lower and upper bounds on mutual velocity cited above correspond to chondrule number densities of 4×10^4 and 40 m^{-3}, respectively, as the chondrules cooled through the 360 to ~580 °C interval. The higher number densities are consistent with the 10^3–10^4 m^{-3} values at temperatures above the silicate solidus based on the abundance of sodium in olivine (Alexander and Ebel, 2012). Meanwhile, the lowest estimates of chondrule number density derived above would imply a decrease in density by at least two orders of magnitude during cooling, suggesting rapid expansion of the chondrule formation region.

The lower number density estimates presented above would be consistent with those predicted in the nebular shock model of chondrule formation for chondrule enrichment ratios

of greater than 1800 relative to the background solid density (Desch and Connolly, 2002). However, such high enrichment ratios would imply heating of the chondrules to >2,000 K, which is inconsistent with the preservation of relict dusty olivine grains. As such, the Semarkona dusty olivine-bearing chondrules likely did not form via the shock mechanism. Alternatively, the lack of an identifiable high-coercivity magnetization in two chondrules may be due to other factors such as the lack of sufficient high-coercivity ferromagnetic grains or the alignment of the chondrule spin axes nearly perpendicular to the background field. In this case, more than 75 percent of chondrules may have avoided collisions during cooling below the Curie temperature, implying lower solid enrichments. Future paleomagnetic analyses of a greater number of chondrules, particularly using thermal demagnetization, are required for more robust constraints on the fraction of chondrule that carry a unidirectional magnetization.

For the impact jetting model of chondrule formation, estimates of inter-chondrule velocities may be complicated by the effect of correlated particle motion. The computation by Johnson et al. (2015) predicts $\geq$4 collisions per hour for each chondrule during the late cooling stage corresponding to our sampled temperature range, which appears inconsistent with the acquisition of a primary NRM in most dusty olivine-bearing chondrules in Semarkona. However, the collision rate and number density estimates in Johnson et al. (2015) were based on modeling jetted material as a disk that expands only in the radial direction. A more realistic model that includes vertical expansion of this disk would likely reduce this collision rate at late times.

The paleomagnetic measurement of a greater number of chondrules with primary ferromagnetic mineralogy and a history of minimal secondary alteration will be necessary to confirm and expand the results discussed here. Studying chondrules from a range of meteorite classes will expand the temporal and spatial coverage of the paleomagnetic record. Although the most reliable record of magnetic fields during chondrule formation so far is derived from dusty olivine chondrules from a single meteorite, the youngest Al–Mg ages of Semarkona chondrules differ from the oldest at the $>4\sigma$ level (Kita et al., 2013), implying that the eight chondrules studied in Fu et al. (2014b) likely sample a number of chondrule formation events over a time span of at least several hundred thousand years. Other chondrite groups, such as the Renazzo-like carbonaceous chondrites, are expected to yield significantly younger chondrules (Schrader et al., 2017), potentially constraining changes in the nebular magnetic field strength through time. The formation of sampled chondrules at multiple ages implies that the sampled space is in excess of the volume of a single chondrule formation event. However, given broad uncertainties in the degree of planetesimal migration within the protoplanetary disk, the spatial coverage of chondrules from single and multiple chondrule groups remains highly uncertain.

12.4 Conclusions and Future Directions

Chondrule paleomagnetism provides unique constraints on the formation mechanism of chondrules as well as on the properties of their cooling environment. Early attempts to measure chondrule magnetization were hindered by the challenges of maintaining mutual orientation, inadequate characterization of the chondrules' ferromagnetic mineralogy, and the lack of suitably sensitive and high–spatial-resolution magnetometers. Advances in paleomagnetic laboratory protocols now permit the mutual orientation of chondrules with better than 5° accuracy (Fu et al., 2014b; Shah et al., 2017), while new magnetometers such as the SQUID

microscope can detect magnetizations as weak as 5×10^{-14} Am^2 (Fu et al., 2017), which are more than a thousand times weaker than those of the first separated chondrules measured from Allende. At the same time, the quantum diamond microscope (QDM; Figure 12.4c) is capable of mapping the distribution of magnetization at ~1 μm spatial resolution, permitting the identification of ferromagnetic carriers and helping to determine the origin of magnetization. Detailed information has also become available for the alteration and metamorphic history of primitive chondrites [e.g., Alexander et al., (1989), Brearley and Krot (2012), Schrader et al. (2015)]. Combined with high-resolution compositional and magnetic mapping, these insights permit the robust identification of primary ferromagnetic phases in chondrules and the isolation of magnetization recording nebular magnetic fields.

Although few published studies so far have used the full complement of these techniques to reach strong conclusions about the origin and paleointensity of single chondrule magnetizations, studies in the near future may be expected to improve the sample statistics of already studied samples, such as Semarkona, and to produce results from a broader range of chondrite groups. At the same time, similar paleomagnetic experiments on nonchondrule inclusions such as igneous CAIs may also extent the coverage of paleomagnetic information to the formation region of these objects. In time, these experiments on chondrules with different formation times may reveal new clues to the mechanism of chondrule formation and the evolution of chondrule production regions through time.

Acknowledgments

We thank X. -N. Bai, A. J. Brearley, J. Gattacceca, A. Johansen, and A. N. Krot for helpful discussions that improved the manuscript. R. R. F. was supported in part by a Postdoctoral Fellowship from the Lamont-Doherty Earth Observatory. B. P. W. thanks the NASA Emerging Worlds (grant NNX15AH72G), the NASA Solar System Exploration and Research Virtual Institute (grant NNA14AB01A), the U. S. Rosetta program, and Thomas F. Peterson Jr. for their generous support.

References

Alexander, C. M. O'D., Barber, D. J., and Hutchison, R. (1989). The microstructure of Semarkona and Bishunpur. *Geochim. Cosmochim. Acta* 53, 3045–3057.

Alexander, C. M. O'D., and Ebel, D. S. (2012). Questions, questions: Can the contradictions between the petrologic, isotopic, thermodynamic, and astrophysical constraints on chondrule formation be resolved? *Meteorit. Planet. Sci*. 47, 1157–1175.

Asphaug, E., Jutzi, M., and Movshovitz, N. (2011). Chondrule formation during planetesimal accretion. *Earth Planet. Sci. Lett*. 308, 369–379.

Bai, X. -N. (2016). Towards a global evolutionary model of protoplanetary disks. *Astrophys. J*. 821, 80.

Bai, X. -N. (2015). Hall effect controlled gas dynamics in protoplanetary disks. II. Full 3D simulations toward the outer disk. *Astrophys. J*. 798, 84.

Bai, X. -N. (2014). Hall-effect-controlled gas dynamics in protoplanetary disks. I. Wind solutions at the inner disk. *Astrophys. J*. 791, 137.

Bai, X. -N. (2011). Magnetorotational-instability-driven accretion in protoplanetary disks. *Astrophys. J*. 739, 1–19.

Bai, X. -N., and Goodman, J. (2009). Heat and dust in active layers of protostellar disks. *Astrophys. J*. 701, 737–755.

Balbus, S. A. (2003). Enhanced angular momentum transport in accretion disks. *Annu. Rev. Astron. Astrophys*. 41, 555–597.

Bitsch, B., Johansen, A., Lambrechts, M., and Morbidelli, A. (2015). The structure of protoplanetary discs around evolving young stars. *Astron. Astrophys*. 575, A28.

Brearley, A. J., and Krot, A. N. (2012). Metasomatism in the early solar system: The record from chondritic meteorites, in: D.E. Harlov and H. Austrheim (Eds.), *Metasomatism and the Chemical Transformation of Rock*., 659–789. Berlin: Springer-Verlag.

Carporzen, L., Weiss, B. P., Elkins-Tanton, L. T., et al. (2011). Magnetic evidence for a partially differentiated carbonaceous chondrite parent body. *Proc. Natl. Acad. Sci. USA* 108, 6386–6389.

Carrera, D., Johansen, A., and Davies, M. B. (2015). How to form planetesimals from mm-sized chondrules and chondrule aggregates. *Astron. Astrophys*. 579, A43.

Ciesla, F. J., Lauretta, D. S., and Hood, L. L. (2004). The frequency of compound chondrules and implications of chondrule formation. *Meteorit. Planet. Sci*. 39, 531–544.

Cuzzi, J. N., and Hogan, R. C. (2003). Blowing in the wind I. Velocities of chondrule-sized particles in a turbulent protoplanetary nebula. *Icarus* 164, 127–138.

Desch, S. J., and Connolly, H. C. (2002). A model of the thermal processing of particles in solar nebula shocks: Application to the cooling rates of chondrules. *Meteorit. Planet. Sci*. 37, 183–207.

Desch, S. J., and Mouschovias, T. C. (2001). The magnetic decoupling of star formation. *Astrophys. J*. 550, 314–333.

Flock, M., Ruge, J. P., Dzyurkevich, N., et al. (2015). Gaps, rings, and non-axisymmetric structures in protoplanetary disks – From simulations to ALMA observations. *Astron. Astrophys*. 574, A68.

Fu, R. R., Lima, E. A., and Weiss, B. P. (2014a). No nebular magnetization in the Allende CV carbonaceous chondrite. *Earth Planet. Sci. Lett*. 404, 54–66.

Fu, R. R., and Weiss, B. P. (2012). Detrital remanent magnetization in the solar nebula. *J. Geophys. Res*. 117, E02003.

Fu, R. R., Weiss, B. P., Lima, E. A., et al. (2014b). Solar nebula magnetic fields recorded in the Semarkona meteorite. *Science*. 346, 1089–1092.

Fu, R. R., Weiss, B. P., Lima, E. A., et al. (2017). Evaluating the paleomagnetic potential of single zircon crystals using Bishop Tuff zircons. *Earth Planet. Sci. Lett*. 458, 1–13.

Gammie, C. F. (1996). Layered accretion in T Tauri disks. *Astrophys. J*. 457, 355–362.

Garrick-Bethell, I., and Weiss, B. P. (2010). Kamacite blocking temperatures and applications to lunar magnetism. *Earth Planet. Sci. Lett*. 294, 1–7.

Glenn, D. R., Fu, R. R., Kehayias, P., et al. (2017). Micrometer-scale magnetic imaging of geological samples using quantum diamond microscopy. *Geochem. Geophys. Geosyst*. 18, 3254–3267.

Guilet, J., and Ogilvie, G. I. (2014). Global evolution of the magnetic field in a thin disc and its consequences for protoplanetary systems. *Mon. Not. R. Astr. Soc*. 441, 852–868.

Hayashi, C. (1981). Structure of the solar nebula, growth and decay of magnetic fields and effects of magnetic and turbulent viscosities on the nebula. *Sup. Prog. Theor. Phys*. 70, 35–53.

Hewins, R. H., Connolly, H. C., Lofgren, G. E., and Libourel, G. (2005). Experimental constraints on chondrule formation. In A. N. Krot, E. R. D. Scott, and B. Reipurth (Eds.), *Chondrites and the Protoplanetary Disk. ASP Conference Series*, 341, 286–316. San Francisco, CA: Astronomical Society of the Pacific.

Johansen, A. (2009). The role of magnetic fields for planetary formation. In K. G. Strassmeier, A. G. Kosovichev, and J. E. Beckman (Eds.), *Cosmic Magnetic Fields: From Planets, to Stars and Galaxies. Proc. IAU Symp*. 259, 119–128. Cambridge, UK: Cambridge University Press.

Johnson, B. C., Minton, D. A., Melosh, H. J., and Zuber, M. T. (2015). Impact jetting as the origin of chondrules. *Nature* 517, 339–341.
Jones, R. H., and Danielson, L. R. (1997). A chondrule origin for dusty relict olivine in unequilibrated chondrites. *Meteorit. Planet. Sci*. 32, 753–760.
Kimura, M., Grossman, J. N., and Weisberg, M. K. (2008). Fe-Ni metal in primitive chondrites: Indicators of classification and metamorphic conditions for ordinary and CO chondrites. *Meteorit. Planet. Sci*. 43, 1161–1177.
Kita, N. T., and Ushikubo, T. (2012). Evolution of protoplanetary disk inferred from 26Al chronology of individual chondrules. *Meteorit. Planet. Sci*. 47, 1108–1109.
Kita, N. T., Yin, Q. -Z., MacPherson, G. J., et al. (2013). ^{26}Al-^{26}Mg isotope systematics of the first solids in the early solar system. *Meteorit. Planet. Sci*. 48, 1–18.
Krot, A. N., Petaev, M. I., Scott, E. R. D., et al. (1998). Progressive alteration in CV3 chondrites: More evidence for asteroidal alteration. *Meteorit. Planet. Sci*. 33, 1065–1085.
Lanoix, M., Strangway, D. W., and Pearce, G. W. (1978). The primordial magnetic field preserved in chondrules of the Allende meteorite. *Geophys. Res. Lett*. 5, 73–76.
Lappe, S. -C. L. L., Harrison, R. J., Feinberg, J. M., and Muxworthy, A. (2013). Comparison and calibration of nonheating paleointensity methods: A case study using dusty olivine. *Geochem. Geophys. Geosyst*. 14, 1–16.
Leroux, H., Libourel, G., Lemelle, L., and Guyot, F. (2003). Experimental study and TEM characterization of dusty olivines in chondrites: Evidence for formation by in situ reduction. *Meteorit. Planet. Sci*. 38, 81–94.
Lesur, G., Kunz, M. W., and Fromang, S. (2014). Thanatology in protoplanetary discs: The combined influence of Ohmic, Hall, and ambipolar diffusion on dead zones. *Astron. Astrophys*. 566, A56.
Levy, E. H., and Araki, S. (1989). Magnetic reconnection flares in the protoplanetary nebula and the possible origin of meteorite chondrules. *Icarus* 81, 74–91.
Levy, E. H., and Sonett, C. P. (1978). Meteorite magnetism and early solar system magnetic fields. In T. Gehrels (Ed.), *Protostars and Planets: Studies of Star Formation and of the Origin of the Solar System*., 516–532. Tucson, AZ: University of Arizona Press.
McNally, C. P., Hubbard, A., Mac Low, M. -M., Ebel, D. S., and D'Alessio, P. (2013). Mineral processing by short circuits in protoplanetary disks. *Astrophys. J*. 767, L2.
Miura, H., Nakamoto, T., and Doi, M. (2008). Origin of three-dimensional shapes of chondrules: I. Hydrodynamics simulations of rotating droplet exposed to high-velocity rarefied gas flow. *Icarus* 197, 269–281.
Nübold, H., and Glassmeier, K. -H. (2000). Accretional remanence of magnetized dust in the solar nebula. *Icarus* 144, 149–159.
Okuzumi, S., Takeuchi, T., and Muto, T. (2014). Radial transport of large-scale magnetic fields in accretion disks. I. Steady solutions and an upper limit on the vertical field strength. *Astrophys. J*. 785, 127.
Schrader, D. L., Connolly, H. C., Lauretta, D. S., et al. (2015). The formation and alteration of the Renazzo-like carbonaceous chondrites III: Toward understanding the genesis of ferromagnesian chondrules. *Meteor. Planet. Sci*. 50, 15–50.
Schrader, D. L., Davidson, J., and McCoy, T. J. (2016a). Widespread evidence for high-temperature formation of pentlandite in chondrites. *Geochim. Cosmochim. Acta* 189, 359–376.
Schrader, D. L., Fu, R. R., and Desch, S. J. (2016b). Evaluating chondrule formation models and the protoplanetary disk background temperature with low-temperature, sub-silicate solidus chondrule cooling rates. *Lunar Planet. Sci. Conf. XLVII*, 1180.
Schrader, D. L., Nagashima, K., Krot, A. N., et al. (2017). Distribution of ^{26}Al in the CR chondrite chondrule-forming region of the protoplanetary disk. *Geochim. Cosmochim. Acta* 201, 375–302.
Shah, J., Bates, H. C., Muxworthy, A. R., et al. (2017). Long-lived magnetism on chondrite parent bodies. *Earth Planet. Sci. Lett*. 475, 106–118.

Shu, F. H., Shang, H., Glassgold, A. E., and Lee, T. (1997). X-rays and fluctuating x-winds from protostars. *Science*. 277, 1475–1479.
Shu, F. H., Shang, H., and Lee, T. (1996). Toward an astrophysical theory of chondrites. *Science*. 271, 1545–1552.
Stepinski, T. F. (1992). Generation of dynamo magnetic fields in the primordial solar nebula. *Icarus* 97, 130–141.
Sugiura, N., Lanoix, M., Strangway, D. W., (1979). Magnetic fields of the solar nebula as recorded in chondrules from the Allende meteorite. *Phys. Earth Planet. Inter*. 20, 342–349.
Sugiura, N., and Strangway, D. W. (1985). NRM directions around a centimeter-sized dark inclusion in Allende. *Proc. Lunar Planet. Sci. Conf. XV*, C729–C738.
Swartzendruber, L. J., Itkin, V. P., and Alcock, C. B. (1991). The Fe-Ni (iron-nickel) system. *J. Phase Equilibria* 12, 288–312.
Tachibana, S., Nagahara, H., and Mizuno, K. (2006). Constraints on cooling rates of chondrules from metal-troilite assemblages. *Lunar Planet. Sci. Conf. XXXVII*.
Takac, M., and Kletetschka, G. (2015). Meteorite movement during deceleration studied analogically with magnetic remanence in the bullet. In AGU Fall Meeting. Abstract # GP43B-1244.
Tauxe, L. (2010). *Essentials of Paleomagnetism*. Berkeley, CA: University of California Press.
Tsuchiyama, A., Shigeyoshi, R., Kawabata, T., et al. (2003). Three-dimensional structures of chondrules and their high-speed rotation. *Lunar Planet. Sci. Conf. XXXIV*.
Turner, N. J., and Sano, T. (2008). Dead zone accretion flows in protostellar disks. *Astrophys. J. Lett*. 679, L131–L134.
Uehara, M., Gattacceca, J., Leroux, H., Jacob, D., and van der Beek, C. J. (2011). Magnetic microstructures of metal grains in equilibrated ordinary chondrites and implications of paleomagnetism of meteorites. *Earth Planet. Sci. Lett*. 306, 241–252.
Uehara, M., and Nakamura, N. (2006). Experimental constraints on magnetic stability of chondrules and the paleomagnetic significance of dusty olivines. *Earth Planet. Sci. Lett*. 250, 292–305.
van der Marel, N., van Dishoeck, E. F., Bruderer, S., et al. (2013). A major asymmetric dust trap in a transition disk. *Science*. 340, 1199–1202.
Villeneuve, J., Chaussidon, M., and Libourel, G. (2009). Homogeneous distribution of ^{26}Al in the Solar System from the Mg isotopic composition of chondrules. *Science*. 325, 985–988.
Wang, H., Weiss, B. P., Bai, X. -N., et al. (2017). Lifetime of the solar nebula constrained by meteorite paleomagnetism. *Science*. 355, 623–627.
Wardle, M. (2007). Magnetic fields in protoplanetary disks. *Astrophys. Sp. Sci*. 311, 35–45.
Wasilewski, P. (1981). New magnetic results from Allende C3(V). *Phys. Earth Planet. Inter*. 26, 134–148.
Wasilewski, P. J., and O'Bryan, M. V. (1994). Chondrule magnetic properties. *Lunar Planet. Sci. Conf. XXV*, 1467.
Weiss, B. P., and Elkins-Tanton, L. T. (2013). Differentiated planetesimals and the parent bodies of chondrites. *Annu. Rev. Earth Planet. Sci*. 41, 21.
Weiss, B. P., Gattacceca, J., Stanley, S., Rochette, P., and Christensen, U. R. (2010). Paleomagnetic records of meteorites and early planetesimal differentiation. *Sp. Sci. Rev*. 152, 341–390.
Weiss, B. P., and Tikoo, S. M. (2014). The lunar dynamo. *Science*. 346, 1246753–1.
Zhu, Z., Stone, J. M., and Rafikov, R. R. (2013). Low-mass planets in protoplanetary disks with net vertical magnetic fields: The planetary wake and gap opening. *Astrophys. J*. 768, 143.